The Astrophysical Journal, 595:L33–L36, 2003 September 20

MILLIMETER OBSERVATIONS OF GRB 030329: CONTINUED EVIDENCE FOR A TWO-COMPONENT JET

Kartik Sheth,[1] Dale A. Frail,[2] Stephen White,[3] Mousumi Das,[3] Frank Bertoldi,[4] Fabian Walter,[2] Shri R. Kulkarni,[1] and Edo Berger[1]

Received 2003 July 3; accepted 2003 August 7; published 2003 August 21

ABSTRACT

We present the results of a dedicated campaign on the afterglow of GRB 030329 with the millimeter interferometers of the Owens Valley Radio Observatory (OVRO) and the Berkeley-Illinois-Maryland Association (BIMA), and with the MAMBO-2 bolometer array on the IRAM 30 m telescope. These observations allow us to trace the full evolution of the afterglow of GRB 030329 at frequencies of 100 and 250 GHz for the first time. The millimeter light curves exhibit two main features: a bright, constant flux density portion and a steep power-law decline. The absence of bright, short-lived millimeter emission is used to show that the GRB central engine was not actively injecting energy well after the burst. The millimeter data support a model, advocated by Berger et al., of a two-component jetlike outflow in which a narrow-angle jet is responsible for the high-energy emission and early optical afterglow, and a wide-angle jet carrying most of the energy is powering the radio and late optical afterglow emission.

Subject headings: cosmology: observations — gamma rays: bursts — radio continuum: general

1. INTRODUCTION

A link between long-duration gamma-ray bursts (GRBs) and the core collapse of massive stars has long been claimed on observational (e.g., Bloom, Kulkarni, & Djorgovski 2002a; Bloom et al. 2002b; Price et al. 2002) and theoretical (Woosley 1993; Paczyński 1998; MacFadyen & Woosley 1999) grounds, but the recent GRB 030329 has strengthened this association considerably. Optical spectra taken of this event (Stanek et al. 2003; Hjorth et al. 2003; Kawabata et al. 2003) showed the usual power-law continuum from the afterglow, superposed upon which were lines characteristic of a Type Ic supernova (SN). Designated SN 2003dh, the brightness of this SNe and its broad line widths are strikingly similar to another peculiar Ic SN 1998bw (Patat et al. 2001; Maeda et al. 2002), or perhaps SN 1997ef (Iwamoto et al. 2000). Depending on the degree of asphericity assumed in modeling the explosion, the derived kinetic energies for SN 1998bw and SN 1997ef are in the range of 5–50 foe (1 foe $= 10^{51}$ ergs). Such events are labeled "hypernovae," an empirical classification to distinguish them from ordinary core collapse SNe with energies of order 1 foe (Iwamoto et al. 1998).

While the nonrelativistic component of the explosion (as traced by SN 2003dh) may have been hyperenergetic, the relativistic component (as traced by GRB 030329) seems to be subenergetic. As noted by Granot, Nakar, & Piran (2003) and Berger et al. (2003b), if the sharp break in the optical light curves at $t = 0.55$ days (Price et al. 2003) is due to a jetlike outflow, then the gamma-ray energy released $E_\gamma \sim 0.05$ foe, and the X-ray luminosity (at $t = 10$ hr) $L_X \sim 3 \times 10^{43}$ ergs s^{-1}. These values of E_γ and L_X lie an order of magnitude or more below which most GRBs are tightly clustered (Bloom, Frail, & Kulkarni 2003; Berger, Kulkarni, & Frail 2003a). Outliers in the energy/luminosity distribution are potentially important for exploring the diversity of the GRB phenomena and how the central engine partitions the explosion energy.

Millimeter detections of GRBs, while difficult to achieve (e.g., Bremer et al. 1998; Shepherd et al. 1998), are a potentially powerful diagnostic of the explosion energy. Since the peak of the synchrotron spectrum is expected to pass through the millimeter band on a timescale of a day or so after the burst (Sari, Piran, & Narayan 1998), such observations are useful for constraining the peak of the spectrum, a quantity that is difficult to obtain by other means. When combined with broadband data these millimeter observations have been especially useful in deriving the kinetic energy of the outflow and the density structure of the circumburst environment (Galama et al. 2000; Berger et al. 2000; Harrison et al. 2001; Yost et al. 2002).

In this Letter we present measurements of GRB 030329 at 100 GHz made with the millimeter interferometers of the Owens Valley Radio Observatory (OVRO) and the Berkeley-Illinois-Maryland Association (BIMA), and measurements at 250 GHz made with MAMBO-2 bolometer array on the IRAM 30 m telescope. At $z = 0.1686$ (Caldwell et al. 2003), this is the closest known GRB, and subsequently the flux density at millimeter wavelengths was more than 10 times brighter than any previous event. These observations allow us to trace the full evolution of the afterglow at millimeter wavelengths for the first time. In § 2 we discuss the observations and calibration issues, and in §§ 3 and 4 we present the results in the form of a light curve and discuss possible interpretations.

2. OBSERVATIONS AND DATA REDUCTION

Millimeter interferometers.—We used the OVRO millimeter array and the BIMA millimeter array to observe the GRB 030329 in a dedicated campaign beginning 2003 March 30 through 2003 April 17. An additional observation was obtained on 2003 April 30.

For the first three nights, when the redshift of the GRB was unknown, we tuned the local oscillator to the CS (2–1) line at a frequency of 97.98 GHz. After that, we tuned to the CO ($J = 1$–0) line redshifted to $z = 0.1686$.

We imaged the continuum flux using the analog correlator at OVRO, which consists of four 1 GHz bands around the LO frequency from ± 0.5–1.5 and ± 2.5–3.5 GHz. The array was

[1] Division of Mathematical and Physical Sciences, California Institute of Technology, Pasadena, CA 91125; kartik@astro.caltech.edu.
[2] National Radio Astronomy Observatory, P.O. Box O, Socorro, NM 87801.
[3] Department of Astronomy, University of Maryland, College Park, MD 20742-2421.
[4] Max-Planck-Institut für Radioastronomie, Auf dem Hügel 69, D-53121 Bonn, Germany.

TABLE 1
OBSERVATIONS

UT Day	Beginning UT	End UT	Flux	1 σ rms	Observatory	Comments
2003 Mar 30	02:32	11:10	57.5	0.8	OVRO	
2003 Mar 31	03:48	09:16	60.0	0.9	OVRO	
2003 Apr 1	05:49	10:47	70	6	OVRO	(UV-avg., terrible weather)
2003 Apr 2	01:22	10:39	58.5	1.3	OVRO	
2003 Apr 3	01:59	10:38	48.4	1.3	OVRO	
2003 Apr 4	04:38	09:01	53.9	0.9	OVRO	
2003 Apr 5	04:43	10:30	59	2	BIMA	
2003 Apr 6	04:49	11:33	47	2	BIMA	
2003 Apr 7	...	...	...	...	OVRO	No data, bad weather
2003 Apr 8	02:56	03:17	41	5	BIMA	
2003 Apr 9	04:27	04:49	33	3	BIMA	
2003 Apr 10	03:02	03:29	21	4	BIMA	
	04:55	06:10	25.8	3.1	OVRO	
2003 Apr11	03:44	04:08	22	4	BIMA	
	05:02	06:17	19.7	4.0	OVRO	
2003 Apr 12	01:56	02:25	25	4	BIMA	
2003 Apr 13	...	...	...	...	BIMA	No data, bad weather
2003 Apr 14	04:07	04:30	14	4	BIMA	
2003 Apr 15	08:30	09:18	15	4	BIMA	
2003 Apr 16	04:40	05:28	11	3	BIMA	
2003 Apr 17	03:48	04:28	...	...	BIMA	No data, bad weather
2003 Apr 18–30	...	...	...	...	...	No obs.
2003 Apr 30	04:06	08:15	ND	3	BIMA	Upper limit 3 mJy beam^{-1}

in the H configuration and the projected baselines ranged from 5.5 to 84.0 kλ and the single-sideband system temperatures ranged from 150 to 400 K. The complex instrumental gain was calibrated using the quasar 1159+292 every 15 minutes. The flux of 1159+292 was determined using 3C 273 since no planets were available for an absolute calibration; hence, the resulting uncertainty in the overall flux scale is ~15%. We use a flux of 1.95 Jy for 1195+292 to calibrate all the data. The calibrations were done with the MMA software package (Scoville et al. 1993) imaged using standard routines in MIRIAD (Sault, Teuben, & Wright 1995).

At BIMA we used the 800 MHz digital correlator to map the GRB. BIMA was in the compact (C) configuration and projected baselines ranged from 2.2 to 29.3 kλ. The single-sideband temperatures ranged from 200 to 400 K. The same phase calibrator, 1159+292, was used to calibrate the BIMA data. The results for the continuum flux measurements are summarized in Table 1. At OVRO we used the 1 GHz digital spectrometer, and the new 8 GHz COBRA spectrometer, and at BIMA we used the 800 MHz spectrometer both to search for a redshifted CO spectral line in absorption; we did not detect it.

Millimeter continuum flux from the GRB was detected at $\alpha = 10^{h}44^{m}49\overset{s}{.}95$, $\delta = 21°31'17\overset{''}{.}30$ (J2000). This position is coincident with the radio and optical afterglows. The observing campaign is summarized in Table 1. On the first 3 days, we were also able to track the evolution of the GRB flux within a scan because it was bright. These data are listed in Table 2. The light curve is plotted in Figure 1.

TABLE 2
EARLY TIME EVOLUTION

Day	Beginning UT	End UT	Flux	1 σ rms	Observatory
2003 Mar 30	02:32	04:32	50.9	1.6	OVRO
2003 Mar 30	04:32	06:32	60.0	1.4	OVRO
2003 Mar 30	06:32	08:32	61.7	1.9	OVRO
2003 Mar 30	08:32	11:10	57.6	1.6	OVRO
2003 Mar 31	03:48	05:48	59.6	1.6	OVRO
2003 Mar 31	05:48	07:48	62.3	1.7	OVRO
2003 Mar 31	07:48	09:16	59.3	2.0	OVRO
2003 Apr 2	01:22	04:22	55.4	1.8	OVRO
2003 Apr 2	04:22	07:22	66.5	2.1	OVRO
2003 Apr 2	07:22	10:39	54.6	2.4	OVRO

MAMBO 250 GHz *observations*.—The millimeter continuum measurements were made using the 117 channel MAMBO-2 array (Kreysa et al. 1999) at the IRAM 30 m telescope on Pico Veleta (Spain). MAMBO-2 has a half-power spectral bandwidth of 210 and 290 GHz with an effective frequency of 250 GHz. The beam size on the sky is 10.″7. The sources were observed with a single channel using the standard on-off mode with the telescope secondary chopping in azimuth by 32″ at a rate of 2 Hz.

Observations of GRB 030329 were done on eight different epochs between March 30 and April 20, with integration times on sky ranging between 5 and 17 minutes. The observing conditions were good, with the exception of April 2, when the sky noise was unusually strong. The source was observed at elevations between 56° and 74°, with line of sight opacities at 250 GHz in the range 0.1–0.3.

The pointing and focus were checked frequently on the quasar 1043+241, which is only 3° away from the GRB. Usually, the pointing was found to be stable within ~3″. For the absolute flux calibration a number of calibration sources were observed, mostly CW-Leo, which is near the target. We used a flux calibration factor of 35,000 counts Jy^{-1}, the 1 σ uncertainty of which we estimated to be 10%.

The data were analyzed using the MOPSI software package. Correlated noise was subtracted from each channel using the weighted average signals from the surrounding channels. These data are listed in Table 3, and the light curve is plotted in Figure 1.

3. RESULTS

The 100 and 250 GHz millimeter light curves in Figure 1 exhibit two main features: a bright, constant flux density portion and a steep decline. A power-law fit to the decay gives $\alpha_R = -1.98$ (where $F_\nu \propto t^\alpha$) at 100 GHz and $\alpha_R = -1.68$ at 250 GHz. These values are in excellent agreement with that derived by Price et al. (2003) for the optical decay after

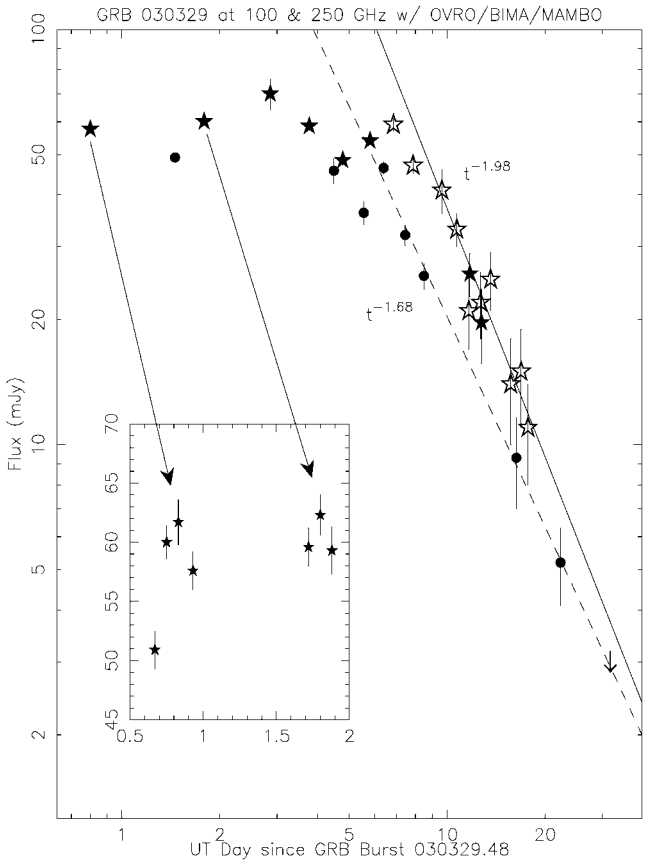

FIG. 1.—Millimeter flux as a function of time on a logarithmic scale. The stars indicate 100 GHz (3 mm) data. Filled stars represent OVRO observations, and open stars represent BIMA observations. Filled circles represent the 250 GHz, IRAM 30 m MAMBO observations. On 2 days (2003 April 10 and April 11), both the BIMA and OVRO observatories observed the GRB. The measurements are consistent with each other. The inset shows the measurements from the first two OVRO epochs, which have been subdivided into 2 hr intervals to look for flux density variations.

~0.5 days ($\alpha_0 = -1.97 \pm 0.12$) and suggests a common physical effect.

The second feature of the light curves in Figure 1 is the bright flux density plateau. In the first week after the burst we derive a mean flux density at 100 GHz of 58 mJy. The emission is constant during this time except for a 2 day period starting on April 2, where there is a small (<20%) but significant drop in the flux density followed by a rise to its mean level on April 5. Likewise, the mean flux density at 250 GHz for the first 4 epochs prior to the decay is 44 mJy. Small variations at 250 GHz during this time are likely due to uncertainties in the calibration.

During the time that these millimeter measurements were made to the optical light curve had a prominent bump at $\Delta t = 1.5$ days with the flux increasing by a factor of 2. There may be a second bump at 3.5 days, but this interpretation depends on whether we compare to a power law with $\alpha = -2$ or -1. In order to search for similar variations at 100 GHz we subdivided each of our observing sessions into 2 hr intervals. The results of this analysis are summarized in Table 2. With the exception of a possible increase by about 10 mJy (15%–20%) at $t \approx 0.7$ day and $t \approx 2.8$ days, neither of which corresponds to a change in the optical brightness, we find no significant variations.

4. DISCUSSION

Two explanations have been offered as to why GRB 030329 appears to be underenergetic compared with other GRBs. Granot et al. (2003) have explained the observed steep decay in the optical light curves of GRB 030329 at $t = 0.55$ days (Price et al. 2003) in terms of a standard model of a jet expanding into a constant density medium (Sari, Piran, & Halpern 1999). Note that such steep temporal breaks $\Delta\alpha > 1$ are not expected in spherical outflows in general, nor are they expected in collimated outflows expanding into a wind-blown medium (Sari et al. 1998; Kumar & Panaitescu 2000). In their model the fluctuations in the optical light curve (§ 3) originate from "refreshed shocks," in which slower moving ejecta catch up with the main shock and reenergize it. In this picture energy injection from the central engine is not instantaneous (as commonly assumed) but episodic, with most of the energy being carried by ejecta with the lower Lorentz factors.

An unavoidable consequence of having the GRB central engine inject a range of Lorentz factors Γ over time, instead of a single high Lorentz factor shell, is that each newly arrived shell at the shock front modifies the afterglow spectrum, producing a short-lived reverse shock, and shifts the combined spectrum to lower frequencies (Rees & Mészáros 1998; Kumar & Piran 2000). According to the more detailed calculations of Sari & Mészáros (2000), which take into account synchrotron self-absorption, there should be a significant enhancement of the flux density at millimeter and submillimeter wavelengths. Short-lived reverse shocks increase the peak flux density by Γ and shift the peak to lower frequencies by a factor of Γ^{-2}. For the Lorentz factors given by Granot et al. (2003) we would have expected to see order-of-magnitude variations in the millimeter flux decaying on timescales of a day or less. This key prediction is contrary to what was seen (§ 3) in our millimeter data and thus our observations rule out the refreshed shock model.

Berger et al. (2003b) proposed a two-component jet model based on the existence of two different jets breaks, one in the

TABLE 3
250 GHz MAMBO OBSERVATIONS

Day	Beginning UT	Int. (s)	Flux	1 σ rms	Comments
2003 Mar 30	22:21	1031	49.2	1.1	Elev. = 74°, τ = 0.21
2003 Apr 2	06:55	156	45.7	3.2	Elev. = 62°, τ = 0.36
2003 Apr 2	23:07	308	36.2	2.3	Elev. = 71°, τ = 0.29
2003 Apr 4	00:29	310	41.6	1.6	Elev. = 56°, τ = 0.13
2003 Apr 4	20:39	312	46.4	1.6	Elev. = 65°, τ = 0.13
2003 Apr 5	21:54	306	32.0	1.8	Elev. = 74°, τ = 0.10
2003 Apr 6	23:17	310	25.5	1.8	Elev. = 67°, τ = 0.10
2003 Apr 14	19:30	468	9.3	2.3	Elev. = 60°, τ = 0.26
2003 Apr 20	19:15	970	5.2	1.1	Elev. = 62°, τ = 0.24

optical light curves at 0.55 days and another best seen in the radio light curves at 9.8 days. Single-jet fits to the radio data could not explain the evolution of the optical emission before 1.5 days, especially the sharp break at 0.55 days (Price et al. 2003). The millimeter observations presented here are crucial in this respect since they define the peak of the synchrotron spectrum and, hence, the overall normalization. Lacking such data, earlier claims of a two-component outflow for GRB 991216 (Frail et al. 2000) are less secure. In this case Berger et al. (2003b) define a narrow-angle jet with $t_{\rm NAJ} = 0.55$ days and $\theta_{\rm NAJ} = 0.09$ rad, which is responsible for the early afterglow, and a wide-angle jet $t_{\rm WAJ} = 9.8$ days and $\theta_{\rm WAJ} = 0.3$ rad, which carries the bulk of the energy in the outflow and dominates the optical and radio emission after ~1.5 days. It is likely that the plateau, seen in the millimeter light curves (§ 3) during the first week, is a combination of the falling flux density (as $t^{-1/3}$) from the NAJ, and a rising flux density (as $t^{1/2}$) from the WAJ (Sari et al. 1999).

Since in the two-component model the flux increase at 1.5 days is due to the rise of the wide-jet component, which then evolves in the usual fashion as $F_\nu \propto t^{-1}$, the subsequent possible fluctuations discussed by Granot et al. (2003) and in § 3 are modest and no longer require refreshed shocks but instead could be explained by variations in the circumburst density.

In summary, the millimeter observations presented here have been used to distinguish between two equally compelling models for GRB 030329 and its afterglow. The absence of bright, short-lived millimeter emission, coincident with "bumps" in the optical light curve between 1 and 7 days after the burst, was used to show that the GRB central engine was not actively injecting energy on this timescale. Instead, the millimeter data support the proposed two-component jet. It is possible that the true structure of GRB outflows are considerably more complicated than the simple picture presented here (Zhang & Mészáros 2002; Rossi, Lazzati, & Rees 2002; Perna, Sari, & Frail 2003). Models of relativistic jets propagating out through the stellar progenitor show that there may exist a large range in Lorentz factors in the outflow (MacFadyen, Woosley, & Heger 2001; Zhang, Woosley, & MacFadyen 2003), which decrease away from the rotation axis as the degree of baryon entrainment increases. Nonetheless, within the limits of the current data for GRB 030329, there is evidence for jet structure with at least two distinct components, with the wider of the two carrying the bulk of the energy. This last point is worth emphasizing since events like GRB 030329/SN 2003dh and GRB 980425/SN 1998bw (Kulkarni et al. 1998) have shown that the group of subenergetic bursts may simply be an artifact of limited observations. True calorimetry of GRBs must account for material at low Lorentz factors (Berger et al. 2003b), which typically are brightest at radio and optical wavelengths.

GRB research at Caltech is supported by grants from NASA and the National Science Foundation. The National Radio Astronomy Observatory is a facility of the National Science Foundation operated under cooperative agreement by Associated Universities, Inc. D. A. F. thanks the Astronomical Institute at the University of Amsterdam for their hospitality during the time when this Letter was written. Research at the OVRO is partially funded by NSF grant AST-9981546 and at BIMA by NSF grant AST-9981289. We acknowledge the support of R. Zylka and A. Weiss in observations with the IRAM 30 m telescope, which is supported by INSU/CNRS (France), MPG (Germany), and IGN (Spain).

REFERENCES

Berger, E., Kulkarni, S. R., & Frail, D. A. 2003a, ApJ, 590, 379
Berger, E., et al. 2000, ApJ, 545, 56
———. 2003b, Nature, in press
Bloom, J. S., Frail, D. A., & Kulkarni, S. R. 2003, ApJ, 594, 674
Bloom, J. S., Kulkarni, S. R., & Djorgovski, S. G. 2002a, AJ, 123, 1111
Bloom, J. S., et al. 2002b, ApJ, 572, L45
Bremer, M., Krichbaum, T. P., Galama, T. J., Castro-Tirado, A. J., Frontera, F., Van Paradijs, J., Mirabel, I. F., & Costa, E. 1998, A&A, 332, L13
Caldwell, N., Garnavich, P., Holland, S., Matheson, T., & Stanek, K. Z. 2003, GRB Circ. Network, 2053, 1
Frail, D. A., et al. 2000, ApJ, 538, L129
Galama, T. J., et al. 2000, ApJ, 541, L45
Granot, J., Nakar, E., & Piran, T. 2003, ApJ, submitted (astro-ph/0304563)
Harrison, F. A., et al. 2001, ApJ, 559, 123
Hjorth, J., et al. 2003, Nature, 423, 847
Iwamoto, K., et al. 1998, Nature, 395, 672
———. 2000, ApJ, 534, 660
Kawabata, K. S., et al. 2003, ApJ, 593, L19
Kreysa, E., et al. 1999, Infrared Phys. Tech., 40, 191
Kulkarni, S. R., et al. 1998, Nature, 395, 663
Kumar, P., & Panaitescu, A. 2000, ApJ, 541, L9
Kumar, P., & Piran, T. 2000, ApJ, 532, 286
MacFadyen, A. I., & Woosley, S. E. 1999, ApJ, 524, 262
MacFadyen, A. I., Woosley, S. E., & Heger, A. 2001, ApJ, 550, 410
Maeda, K., Nakamura, T., Nomoto, K., Mazzali, P. A., Patat, F., & Hachisu, I. 2002, ApJ, 565, 405
Paczyński, B. 1998, ApJ, 494, L45
Patat, F., et al. 2001, ApJ, 555, 900
Perna, R., Sari, R., & Frail, D. A. 2003, ApJ, 594, 379
Price, P. A., et al. 2002, ApJ, 572, L51
———. 2003, Nature, 423, 824
Rees, M. J., & Mészáros, P. 1998, ApJ, 496, L1
Rossi, E., Lazzati, D., & Rees, M. J. 2002, MNRAS, 332, 945
Sari, R., & Mészáros, P. 2000, ApJ, 535, L33
Sari, R., Piran, T., & Halpern, J. P. 1999, ApJ, 519, L17
Sari, R., Piran, T., & Narayan, R. 1998, ApJ, 497, L17
Sault, R. J., Teuben, P. J., & Wright, M. C. H. 1995, in ASP Conf. Ser. 77, Astronomical Data Analysis Software and Systems IV, ed. R. A. Shaw, H. E. Payne, & J. J. E. Hayes (San Francisco: ASP), 433
Scoville, N. Z., Carlstrom, J. E., Chandler, C. J., Phillips, J. A., Scott, S. L., Tilanus, R. P. J., & Wang, Z. 1993, PASP, 105, 1482
Shepherd, D. S., Frail, D. A., Kulkarni, S. R., & Metzger, M. R. 1998, ApJ, 497, 859
Stanek, K. Z., et al. 2003, ApJ, 591, L17
Woosley, S. E. 1993, ApJ, 405, 273
Yost, S. A., et al. 2002, ApJ, 577, 155
Zhang, B., & Mészáros, P. 2002, ApJ, 571, 876
Zhang, W., Woosley, S. E., & MacFadyen, A. I. 2003, ApJ, 586, 356